



## A simple calculation algorithm to separate high-resolution CH<sub>4</sub> flux measurements into ebullition and diffusion-derived components

Mathias Hoffmann<sup>1,\*</sup>, Maximilian Schulz-Hanke<sup>2</sup>, Juana Garcia Alba<sup>1</sup>, Nicole Jurisch<sup>2</sup>, Ulrike  
5 Hagemann<sup>2</sup>, Torsten Sachs<sup>3</sup>, Michael Sommer<sup>1,4</sup>, Jürgen Augustin<sup>2</sup>

<sup>1</sup>Institute of Soil Landscape Research, Leibniz Centre for Agricultural Landscape Research (ZALF) e.V., Eberswalder Str. 84, 15374 Müncheberg, Germany

<sup>2</sup>Institute for Landscape Biogeochemistry, Leibniz Centre for Agricultural Landscape  
10 Research (ZALF) e.V., Eberswalder Str. 84, 15374 Müncheberg, Germany

<sup>3</sup>GFZ German Research Centre for Geosciences, Telegrafenberg, 14473 Potsdam, Germany

<sup>4</sup>University of Potsdam, Institute of Earth and Environmental Sciences, Karl-Liebknecht-Str.  
24-25, 14476 Potsdam, Germany

15

\*Corresponding author:

Mathias Hoffmann (Mathias.Hoffmann@zalf.de)

<sup>1</sup>Institute of Soil Landscape Research, Leibniz Centre for Agricultural Landscape Research (ZALF) e.V.

20 Eberswalder Str. 84, 15374 Müncheberg, Germany

E-mail: Mathias.hoffmann@zalf.de

Tel.: +49(0)33432 82 327

Fax: +49(0)33432 82 280

25

30



### Abstract

35 Processes driving the production, transformation and transport of methane (CH<sub>4</sub>) in wetland  
ecosystems are highly complex. We present a simple calculation algorithm to separate open-  
water CH<sub>4</sub> fluxes measured with automatic chambers into diffusion- and ebullition-derived  
components. This helps to reveal underlying dynamics, to identify potential environmental  
drivers, and thus, calculate reliable CH<sub>4</sub> emission estimates. The flux separation is based on  
40 identification of ebullition-related sudden concentration changes during single measurements.  
Therefore, a variable ebullition filter is applied, using the lower and upper quartile and the  
interquartile range (IQR). Automation of data processing is achieved by using an established  
R-script, adjusted for the purpose of CH<sub>4</sub> flux calculation. The algorithm was tested using flux  
measurement data (July to September 2013) from a former fen grassland site, converted into a  
45 shallow lake as a result of rewetting. Ebullition and diffusion contributed equally (46 % and  
55 %) to total CH<sub>4</sub> emissions, which is comparable to ratios given in literature. Moreover, the  
separation algorithm revealed a concealed shift in the diurnal trend of diffusive fluxes  
throughout the measurement period. The water temperature gradient was identified as one of  
the major drivers of diffusive CH<sub>4</sub> emissions, whereas no significant driver was found in case  
50 of erratic CH<sub>4</sub> ebullition events.

### Keywords

Wetland ecosystems, ebullition, diffusion, automatic chamber system, diurnal variability, R-  
script

55

60

65



## 1. Introduction

Wetlands and freshwaters are among the main sources for methane ( $\text{CH}_4$ ) emissions (Dengel et al. 2013; Bastviken et al. 2011; IPCC 2013). In open-water systems,  $\text{CH}_4$  is released via three main pathways: i) diffusion (including “storage flux”, in terms of rapid diffusive release  
70 from methane stored in the water column), ii) ebullition and iii) plant-mediated transport (e.g., Goodrich et al. 2011; Bastviken et al. 2004; Van der Nat and Middelburg 2000; Whiting and Chanton 1996). The magnitude of  $\text{CH}_4$  released via the different pathways is subject to variable environmental drivers and conditions such as water level, atmospheric pressure, temperature gradients, wind velocity, and the presence of macrophytes (Lai et al. 2012;  
75 Tokida et al. 2007; Chanton and Whiting 1995). As particularly ebullition varies in time and space (Maeck et al. 2013; Walter et al. 2006), total  $\text{CH}_4$  emissions feature an extremely high spatial and temporal variability at all scales (Koch et al. 2014; Repo et al. 2007; Bastviken et al. 2004). Hence, attempts to model  $\text{CH}_4$  emissions based on individual environmental drivers are highly complex. The separation of measured  $\text{CH}_4$  emissions into the individual pathway-associated components is therefore crucial if aiming to identify relevant environmental drivers  
80 of  $\text{CH}_4$  emissions (Bastviken et al. 2011; Bastviken et al. 2004). In consequence, the understanding of the complex processes determining the temporal and spatial patterns of  $\text{CH}_4$  emissions is a prerequisite for upscaling field-measured  $\text{CH}_4$  emissions to the landscape or regional scale, and thus for adequately quantifying the contribution of wetland  $\text{CH}_4$  emissions  
85 to global greenhouse gas (GHG) budgets (Walter et al. 2015; Koebisch et al. 2015; Lai et al. 2012; Limpens et al. 2008).

However, field studies measuring  $\text{CH}_4$  release above shallow aquatic environments or flooded peatlands generally measure total  $\text{CH}_4$  emissions as a mixed signal of individual  $\text{CH}_4$  emission components, released via all possible pathways (i.e. diffusion, ebullition and plant-mediated transport). Studies separately measuring temporal and spatial patterns of  $\text{CH}_4$   
90 emissions resulting only from either ebullition or diffusion are rare. Measurements of  $\text{CH}_4$  ebullition can be performed using manual or automatic gas traps, as well as optical and hydro-acoustic methods (Wik et al. 2013; Maeck et al. 2013; Wik et al. 2011; Walter et al. 2008; Ostrovsky et al. 2008; Huttunen et al. 2001; Chanton and Whiting 1995), often requiring  
95 considerable instrumentation within the studied system. Diffusive  $\text{CH}_4$  fluxes are commonly either derived indirectly as the difference between total  $\text{CH}_4$  emissions and measured ebullition, or directly obtained based on the use of bubble shields or gradient measurements of  $\text{CH}_4$  concentration differences (DelSontro et al. 2011; Bastviken et al. 2010; Bastviken et al. 2004). A graphical method to separate diffusion, steady ebullition and episodic ebullition



100 fluxes from the total CH<sub>4</sub> flux was presented by Yu et al. (2014), using a flow-through  
chamber system. However, performed at the laboratory scale for a peat monolith,  
measurement results as well as the applied method were lacking direct field applicability. A  
first simple mathematical approach for field measurements to separate ebullition from the sum  
of diffusion and plant-mediated transport was introduced by Miller and Oremland (1988),  
105 who used low-resolution static chamber measurements. Goodrich et al. (2011) specified the  
approach using piecewise linear fits for single ebullition events. However, static thresholds  
determining ebullition events, as well as low-resolution measurements, limited the approach  
to estimates of medium and major ebullition events and prevented a clear flux separation.  
Therefore, CH<sub>4</sub> flux separation approaches based on manual chamber measurements with  
110 rather low temporal resolution fail to capture the rapidly changing absolute and relative  
contributions of the pathway-associated flux components both in time and space (Maeck et al.  
2013; Walter et al. 2006).

Hence, there is a need for a non-intrusive method for separating pathway-associated CH<sub>4</sub> flux  
components both in time and space. Improvements in measurement techniques, particularly  
115 by using high-resolution gas analyzers (e.g., within Eddy Covariance (EC) measurements),  
allow for high temporal resolution records of CH<sub>4</sub> emissions (Schrier-Uijl et al. 2011; Wille et  
al. 2008). Recently, a growing number of experimental GHG studies employ automatic  
chambers (AC) (Koskinen et al. 2014; Lai et al. 2014; Ramos et al. 2006), which can provide  
flux data with an enhanced temporal resolution and capture short-term temporal (e.g., diurnal)  
120 dynamics. In addition, AC measurements can also represent small-scale spatial variability,  
and thus identify potential hot spots of CH<sub>4</sub> emissions (Koskinen et al. 2014; Lai et al. 2014).  
AC systems therefore combine the advantages of chamber measurements and  
micrometeorological methods with respect to the quantification of spatial as well as temporal  
dynamics of CH<sub>4</sub> emissions (Savage et al. 2014; Lai et al. 2012).

125 Combined with a high-resolution gas analyzer (e.g., cavity ring-down spectroscopy), AC  
measurements provide opportunities for i) detecting even minor ebullition events, and ii)  
developing a statistically based flux separation approach. This study presents a new  
calculation algorithm for separating open-water CH<sub>4</sub> fluxes into its ebullition- and diffusion-  
derived components based on ebullition-related sudden concentration changes during  
130 chamber closure. A variable ebullition filter is applied using the lower and upper quartile and  
the interquartile range (IQR) of measured concentration changes. Data processing is based on  
the R-script developed by Hoffmann et al. (2015), modified for the purpose of CH<sub>4</sub> flux



calculation and separation, thus including the advantages of automated and standardized flux  
estimation. We hypothesize that the presented flux calculation and separation algorithm can  
135 reveal concealed spatial and temporal dynamics in ebullition- and diffusion-associated CH<sub>4</sub>  
fluxes, thus facilitating the identification of relevant environmental drivers.

## 2. Material and Methods

### 2.1 Exemplary field data

#### 140 2.1.1 Study site

Ecosystem CH<sub>4</sub> exchange was measured at a flooded former fen grassland site, located within  
the Peene river valley in Mecklenburg-Western Pomerania, northeast Germany (53°52'N,  
12°52'E). The long-term annual precipitation is 570 mm. The mean annual air temperature is  
8.7°C (DWD, Anklam). The study site was particularly influenced by a complex melioration  
145 and drainage program between 1960 and 1990, characterized by intensive agriculture. As a  
consequence, the peat layer was degraded and the soil surface was lowered by subsidence.  
Being included in the Mecklenburg-Western Pomerania Mire Restoration Program, the study  
site was rewetted at the beginning of 2005. As a result, the water level was permanently above  
the soil surface, thus transforming the site into a shallow lake. Exceptionally high CH<sub>4</sub>  
150 emissions at the measurement site are reported by Franz et al. (2016), who measured CO<sub>2</sub> and  
CH<sub>4</sub> emissions using an eddy covariance system and Hahn-Schöffl et al. (2011), who  
investigated sediments formed during inundation. Prior to rewetting, the vegetation was  
dominated by reed canary grass (*Phalaris arundinacea*), which disappeared after rewetting  
due to permanent inundation. At present, the water surface is partially covered with duckweed  
155 (Lemnoideae), while broadleaf cattail (*Typha latifolia*) and reed mannagrass (*Glyceria  
maxima*) are present next to the shoreline. However, below chambers, no emergent  
macrophytes were present throughout the study period.

#### 2.1.2 Automatic chamber system

160 In April 2013, the measurement site was equipped with an AC system and a nearby climate  
station (Fig. 1). The AC system consists of four transparent chambers, installed as transect  
from the shoreline into the lake. Chambers are made of Lexan Polycarbonate with a thickness  
of 2 mm and reinforced with an aluminium frame. Each chamber (volume of 1.5 m<sup>3</sup>; base area  
1 m<sup>2</sup>) is mounted in a steel profile, secured by wires, and lifted/lowered by an electronically



165 controlled cable winch located at the top of the steel profile. All chambers are equipped with a  
water sensor (capacitive limit switch KB 5004, efactor150) at the bottom, which allows  
steady immersion (5 cm) of the chambers into the variable water surface. Hence, airtight  
sealing as well as constant chamber volume are ensured during the study period. All chambers  
are connected by two tubes and a multiplexer to a single Los Gatos Fast Greenhouse Gas  
170 Analyser (911-0010, Los Gatos), measuring the air concentration of carbon dioxide (CO<sub>2</sub>),  
methane (CH<sub>4</sub>), and water vapour (H<sub>2</sub>O). To ensure consistent air pressure and mixture during  
measurements, chambers are ventilated by a fan and sampled air is transferred back into the  
chamber headspace. However, due to the large chamber volume, complete mixture of the  
chamber headspace took up to 30 seconds. In consequence, most peaks due to ebullition  
175 events showed overcompensation (Fig. 3). Concentration measurements are performed in  
sequence, sampling each chamber for 10 minutes with a 15-second frequency once per hour.  
A wooden boardwalk north of the measurement site allows for maintenance access, while  
avoiding disturbances of the water body and peat surface.

### 180 2.1.3 Ancillary field measurements

Temperatures were recorded in different water (5 cm above sediment surface) and sediment  
depths (2 cm, 5 cm, and 10 cm below the sediment-water interface), using thermocouples  
(T107, Campbell Scientific). Additionally, air temperature at 20 cm and 200 cm height, as  
well as wind speed, wind direction, precipitation, relative humidity, and air pressure were  
185 measured by a nearby climate station (WXT52C, Vaisala). Water table depth was measured  
by a pressure probe (PDCR1830, Campbell Scientific). All parameters were continuously  
recorded at 30-minute intervals and stored by a data logger (CR 1000, Campbell Scientific)  
connected to a GPRS radio modem.

### 190 2.2 Flux calculation and separation algorithm

CH<sub>4</sub> flux calculation was performed using a standardized R-script presented in detail by  
Hoffmann et al. (2015). Measured fluxes were determined using Eq. (1), where M is the  
molar mass of CH<sub>4</sub>,  $\delta v$  is the linear concentration change over time (t), A and V denote the  
basal area and chamber volume, respectively, and T and P represent the inside air temperature  
and air pressure. R is a constant (8.3143 m<sup>3</sup> Pa K<sup>-1</sup> mol<sup>-1</sup>).  
195

$$r_{\text{CH}_4} (\mu\text{mol C m}^{-2} \text{ s}^{-1}) = \frac{M * P * V * \delta v}{R * T * t * A} \quad (1)$$



To estimate the relative contribution of diffusion and ebullition to total CH<sub>4</sub> emissions, flux calculation was performed twice, adjusting selected user-defined parameter setups of the used R-script (Hoffmann et al. 2015) (Fig. 3). First, the diffusive component of the flux rate ( $CH_{4_{diffusion}}$ ) was calculated based on a variable moving window (MW) with a minimum size of 5 consecutive data points. Abrupt concentration changes within the MW were identified by means of a rigid outlier test, discarding fluxes with an inherent concentration change larger or smaller than the upper and lower quartile  $\pm 0.25$  times the interquartile range (IQR). Tests of variance homogeneity and normal distribution were applied with  $\alpha=0.1$ . Second, the total CH<sub>4</sub> flux ( $CH_{4_{total}}$ ) for each measurement was calculated as the difference between the start and end CH<sub>4</sub> concentration using an enlarged MW with a minimum length of 7.5 minutes. To avoid measurement artefacts (e.g., overcompensation), being taken into account as start or end concentration, measurement points representing an inherent concentration change smaller or larger than the upper and lower quartile  $\pm 0.25$  times IQR were discarded prior to calculation of the total CH<sub>4</sub> flux. Third, the proportion of the total CH<sub>4</sub> emission released via ebullition was estimated following Eq. (2).

$$CH_{4_{ebullition_n}} = \sum_{i=1}^n (CH_{4_{total}} - CH_{4_{diffusion}}) \quad (2)$$

Since no emergent macrophytes were present below the automatic chambers, plant-mediated transport of CH<sub>4</sub> was assumed to be zero. The same accounts for negative estimates of CH<sub>4</sub> released through ebullition. To exclude measurement artefacts triggered by the process of closing the chamber, a death band of 25 % was applied to the beginning of each measurement prior to all flux calculation steps. The used R-script, a manual and test dataset are available at <https://zenodo.org/record/53168>.

220

### 2.3 Verification of applied flux separation algorithm

A laboratory experiment under reasonable controlled conditions was performed to verify the used flux separation algorithm. In order to artificially simulate ebullition events, distinct amounts (5, 10, 20, 30 and 50 ml) of a gaseous mixture (25 000 ppm CH<sub>4</sub> in artificial air; Linde, Germany) were inserted by a syringe through a pipe into a water filled tub covered with a closed chamber ( $V=0.114 \text{ m}^3$ ;  $A= 0.145 \text{ m}^2$ ). Airtight sealing was ensured by a water-filled frame connecting tub and chamber. The chamber was ventilated by a fan and connected via pipes to a Los Gatos Greenhouse Gas Analyser (911-0010, Los Gatos), measuring CH<sub>4</sub> concentrations inside the chamber with a 1 Hz frequency (Fig. 2). To ensure comparability



230 between *in vitro* and *in situ* measurements, data processing was performed based on 0.066 Hz records. The expected concentration changes within the chamber headspace as the result of methane injections was calculated as the mixing ratio between the amount of inserted gaseous mixture (25 000 ppm) and the air filled chamber volume (2 ppm).

### 235 3. Results and Discussion

The assumption of using sudden changes in chamber-based CH<sub>4</sub> concentration measurements to detect ebullition events was verified by the conducted laboratory experiment. Calculations of the simulated ebullition events and the amount of injected CH<sub>4</sub> showed a good overall agreement, which indicates the accuracy of the calculation algorithm (Fig. 4). However, flux separation might be hampered due to a steady flux originating from other processes than diffusion through peat and water layers, such as the steady ebullition of micro bubbles (Prairie and del Giorgio 2013; Goodrich et al. 2011). A potential resulting impact on estimates of diffusive CH<sub>4</sub> emissions can be minimized by an enhanced frequency of concentration measurements during chamber closure. Based on a high temporal resolution, small-scale differences within measured concentration changes can be identified and filtered by the variable IQR-criterion, which thereby reduces the detection limit of ebullition events. Compared to direct measurements of either diffusion or ebullition, as reported by e.g. Bastviken et al. (2010), the presented calculation algorithm prevents an interfering influence of spatial heterogeneity on separated ebullition and diffusion CH<sub>4</sub> fluxes, since both flux components are derived during the same measurement and the same spatial entity. Moreover, the integration of the ebullition component into measurements rather than the calculation of single ebullition events ensure a reliable flux separation despite of potential measurement artefacts such as overcompensation or incomplete ebullition records (Goodrich et al. 2011; Miller and Oremland 1988). In case of a low water level, such as within the presented study (<35cm) or parallel measurements of different trace gases (e.g., CO<sub>2</sub> and CH<sub>4</sub>), the use of direct measurement systems for either ebullition (gas traps, funnels) or diffusion (bubble shields) might be limited. Hence, the presented simple and robust calculation algorithm, which is purely based on data processing, seems to be applicable to a broader range of different manual and automatic closed chamber systems, instrumental setups, study designs, and ecosystems.

Due to the performed flux separation, the accuracy of temporal tendencies within the exemplary field data set was improved (Fig. 4, Tab. 1) and explanatory approaches could be



addressed. Total CH<sub>4</sub> emissions spatially integrated over the study period, as well as the  
respective contributions of ebullition and diffusion are shown in Fig. 5. Apart from short-term  
265 measurement gaps, a considerable loss of data occurred between the 27<sup>th</sup> of July and 7<sup>th</sup> of  
August 2013 due to malfunction of the measurement equipment.

In general, biochemical processes driving CH<sub>4</sub> production are closely related to temperature  
regimes (Christensen et al. 2005), determining the CH<sub>4</sub> production within the sediment  
(Bastviken et al. 2004). Hence, measured total CH<sub>4</sub> emissions showed distinct seasonal  
270 patterns following the temperature regime at 10 cm sediment depth. In addition to seasonality,  
total CH<sub>4</sub> emissions also featured diurnal dynamics, with lower fluxes during daytime and  
higher fluxes during nighttime, which were most pronounced during July and early September  
(Fig. 5). Especially during August, the diurnal variability was superimposed by short-term  
emission events and high amplitudes in recorded total CH<sub>4</sub> emissions. Similar to total CH<sub>4</sub>  
275 emissions, diffusive fluxes also showed a distinct temperature-driven seasonality as well as  
clear diurnal patterns throughout the entire study period (Fig. 6). However, compared to the  
diurnal variability of the total CH<sub>4</sub> fluxes, a pronounced shift of maximum CH<sub>4</sub> emissions  
from night- to daytime was revealed for the diffusive flux component (Fig. 5, Fig. 6). While  
maximum diffusive fluxes during July were recorded during nighttime hours (approx. 21:00  
280 to 6:00), a shift to the daytime started in August, with maximum fluxes in September  
occurring between 0:00 and 11:00 (Fig. 6). This might be explained by differences in  
turbulent mixing due to changing water temperature gradients. During daytime, the surface  
water is warmed, thus preventing an exchange with the CH<sub>4</sub>-enriched water near the  
sediment, which results in lower diffusive CH<sub>4</sub> emissions. During night time, when the upper  
285 water layer cools down and mixing is undisturbed, enhanced diffusive CH<sub>4</sub> emissions can be  
detected. This dynamics are more pronounced during warm days, explaining the seasonal  
shift, and concealed during periods with a high wind velocity. The obtained diurnal trend is in  
accordance with findings of Sahlée et al. (2014) and Lai et al. (2012), who reported higher  
night time and lower daytime CH<sub>4</sub> emissions for a lake site in Sweden and an ombrotropic  
290 bog in Canada, respectively. However, an opposing tendency was found by Deshmukh et al.  
(2014), who reported higher daytime and lower night time CH<sub>4</sub> emissions from a newly  
flooded subtropical freshwater hydroelectric reservoir within the Lam Theun river valley,  
Laos. In contrast to diurnal trends obtained for the total as well as diffusive CH<sub>4</sub> emissions,  
estimated ebullition events occurred erratically and showed neither clear seasonal nor diurnal  
295 dynamics. Nonetheless, periods characterized by more pronounced ebullition seemed to  
roughly follow the sediment temperature-driven CH<sub>4</sub> production within the sediment as e.g.



reported by Bastviken et al. 2004 (Fig. 5). This is confirmed by a distinct correlation between daily mean sediment temperatures and corresponding sums of measured ebullition fluxes. Moreover, fewer and smaller ebullition events were detected in times of reduced wind velocity and high relative humidity (RH), for example from 10<sup>th</sup>-11<sup>th</sup> September and 18<sup>th</sup>-19<sup>th</sup> 300 September 2013. However, at the level of single flux measurements, no significant dependency was found between the recorded environmental drivers and CH<sub>4</sub> release via ebullition. The relative contributions of diffusion and ebullition were 55 % (min. 33 % to max. 70 %) and 46 % (min. 30 % to max. 67 %), respectively. This is in accordance with 305 values reported by Bastviken et al. (2011), who compiled CH<sub>4</sub> emission estimates from 474 freshwater ecosystems with clearly defined emission pathways. A similar ratio was also found by Tokida et al. (2007), who investigated the role of decreasing atmospheric pressure as a trigger for CH<sub>4</sub> ebullition events in peatlands.

Comparison of flux data among the four chambers reveals considerable spatial heterogeneity 310 within the measured transect (*data not shown*). Monthly averages of diffusive, ebullative and total CH<sub>4</sub> emissions for all four chambers of the established transect as well as statistics showing the explanatory power of different environmental variables are summarized in Tab. 1. With respect to total CH<sub>4</sub> emissions, neighbouring chambers generally featured high differences in CH<sub>4</sub> fluxes, with no obvious trend along the transect. The same holds to be true 315 for derived ebullative and diffusive CH<sub>4</sub> flux components. After separation into diffusion and ebullition, dependencies with respect to different environmental drivers were revealed (Tab. 1).

#### 4. Conclusions

320 The results of the laboratory experiment as well as the estimated relative contributions of ebullition and diffusion during the field study indicate that the presented algorithm for CH<sub>4</sub> flux calculation and separation into diffusion and ebullition delivers reasonable and robust results. Temporal dynamics, spatial patterns and relations with environmental parameters well established in the scientific literature, such as sediment temperature, water temperature 325 gradients and wind velocity, became more pronounced when analysed separately for diffusive CH<sub>4</sub> emissions and ebullition. However, not all ebullition events (e.g., micro bubbles) seemed to be filtered correctly, as detected in case of enhanced CH<sub>4</sub> emissions during the beginning of August and the thereby superimposed diurnal cycling. Hence, further adaptation of measurement frequency and/or the applied data processing algorithm is required. In a next



330 step, the flux separation algorithm should be systematically tested against flux estimates  
generated with methods for measuring either ebullition or diffusion, such as bubble traps or  
bubble barriers. Moreover, the algorithm needs to be tested and evaluated with regards to  
generalizability and applicability to other freshwater and wetland ecosystems. Despite the  
mentioned shortcomings, the presented calculation approach for separating CH<sub>4</sub> emissions  
335 increases the amount of information about the periodicity of CH<sub>4</sub> release and may help to  
reveal the influence of potential drivers as well as to explain temporal and spatial variability  
within both separated flux components.

#### **Acknowledgment**

340 This work was supported by the interdisciplinary research project CarboZALF, the Helmholtz  
Association of German Research Centres through a Helmholtz Young Investigators Group  
grant to T. S. (grant VH-NG-821), and infrastructure funding through the Terrestrial  
Environmental Observatories Network (TERENO). The authors want to express their special  
thanks to Mr. Marten Schmidt for construction as well as continuous maintenance of the auto-  
345 chamber system and creative solutions for all kind of technical problems. The authors are also  
thankful to Mr. Bertram Gusovius for his kind help during performance of the lab experiment.

350

355

360 **References:**

- Bastviken, D., Cole, J. J., Pace, M. L., Tranvik, L. J.: Methane emissions from lakes: Dependence of lake characteristics, two regional assessments, and a global estimate. *Glob. Biogeochem. Cycle* 18, 1-12, 2004.
- Bastviken, D., Santoro, A. L., Marotta, H., Queiroz Pinho, L., Fernandes Calheiros, D., Crill, P.,  
365 Enrich-Prast, E.: Methane Emissions from Pantanal, South America, during the low water season: towards more comprehensive sampling. *Environ. Sci. Technol.* 44, 5450-5455, 2010.
- Bastviken, D., Tranvik, L. J., Downing, J. A., Crill, P. M., Enrich-Prast, A.: Freshwater methane emissions offset the continental carbon sink. *Science* 331, 1, 2011.
- Chanton, J. P., Whiting, G., J.: Trace gas exchange in freshwater and coastal marine environments:  
370 ebullition and transport by plants. In: Matson, P. A., Hariss, R. C. (eds) *Biogenic trace gases: measuring emissions from soil and water*. Blackwell Science Ltd., UK, Chapter 4, 98-125, 1995.
- Christensen, T. R., Ekberg, A., Ström, L., Mastepanov, M., Panikov, N.: Factors controlling large scale variations in methane emissions from wetlands. *Geophys. Res. Lett.* 30, 1-4, 2005
- 375 DelSontro, T., Kunz, M. J., Kempster, T., Wüest, A., Wehrli, B., Senn, D. B.: Spatial heterogeneity of methane ebullition in a large tropical reservoir. *Environ. Sci. Technol.* 45, 9866-9873, 2011
- Dengel, S., Zona, D., Sachs, T., Aurela, M., Jammet, M., Parmentier, F. J. W., Oechel, W., Vesala, T.: Testing the applicability of neural networks as a gap-filling method using CH<sub>4</sub> flux data from high latitude wetlands. *Biogeosciences* 10, 8185-8200, 2013.
- 380 Deshmukh, C., Serca, D., Delon, C., Tardif, R., Demarty, M., Jarnot, C., Meyerfeld, Y., Chanudet, V., Guédant, P., Rode, W., Descloux, S., Guérin, F.: Physical controls on CH<sub>4</sub> emissions from a newly flooded subtropical freshwater hydroelectric reservoir: Nam Theun 2. *Biogeosciences* 11, 4251-4269, 2014.
- Franz, D., Koebsch, F., Larmanou, E., Augustin, J., Sachs, T.: High net CO<sub>2</sub> and CH<sub>4</sub> release at a  
385 eutrophic shallow lake on a formerly drained fen. *Biogeosciences* 13, 3051-3070, 2016.
- Goodrich, J. P., Varner, R. K., Frohling, S., Duncan, B. N., Crill, P. M.: High-Frequency measurements of methane ebullition over a growing season at a temperate peatland site. *Geophys. Res. Lett.* 38, 1-5, 2011.



- Hahn-Schöfl, M., Zak, D., Minke, M., Gelbrecht, J., Augustin, J., Freibauer, A.: Organic sediment  
390 formed during inundation of a degraded fen grassland emits large fluxes of CH<sub>4</sub> and CO<sub>2</sub>.  
Biogeosciences 8, 1539-1550, 2011.
- Hoffmann, M., Jurisch, N., Albiac Borraz, E., Hagemann, U., Drösler, M., Sommer, M., Augustin, J.:  
Automated modeling of net ecosystem exchange based on periodic closed chamber  
measurements: A standardized conceptual and practical approach. Agric.For. Meteorol. 200,  
395 30-45, 2015.
- Huttunen, J. T., Lappalainen, K. M., Saarijärvi, E., Väisänen, T., Martikainen, P. J.: A novel sediment  
gas sampler and a subsurface gas collector used for measurement of the ebullition of methane  
and carbon dioxide from a eutrophied lake. Sci. Total Environ., 266, 153-158, 2001.
- IPCC: Summary for Policymakers. In: Climate Change 2013, The Physical Science Basis, Working  
400 Group I Contribution to the Fifth Assessment Report of the Intergovernmental Panel on  
Climate Change, edited by: Stocker, T. F., Qin, D., Plattner, G.-K., Tignor, M. M. B., Allen,  
S. K., Boschung, J., Nauels, A., Xia, Y., Bex, V., Midgley, P. M., Cambridge University  
Press, Cambridge, United Kingdom and New York, NY, USA, 2013.
- Juszczak, R., Augustin, J.: Exchange of the greenhouse gases methane and nitrous oxide between the  
405 atmosphere and a temperate peatland in central Europe. Wetlands 33, 895-907, 2013
- Koch, S., Jurasinski, G., Koebsch, F., Koch, M., Glatzel, S.: Spatial variability of annual estimates of  
methane emissions in a Phragmites Australis (Cav.) Trin. Ex Steud. dominated restored  
brakish fen. Wetlands 34, 593-602, 2014.
- Koebsch, F., Jurasinski, G., Koch, M., Hofmann, J., Glatzel, S.: Controls for multi-scale temporal  
410 variation in ecosystem methane exchange during the growing season of a permanently  
inundated fen. Agric. For. Meteorol. 204, 94-105, 2015.
- Koskinen, M., Minkinen, K., Ojanen, P., Kämäräinen, M., Laurila, T., Lohila, A.: Measurements of  
CO<sub>2</sub> exchange with an automated chamber system throughout the year: challenges in  
measuring night-time respiration on porous peat soil. Biogeosciences 11, 347-363, 2014.
- 415 Lai, D. Y. F., Roulet, N. T., Moore, T. R.: The spatial and temporal relationship between CO<sub>2</sub> and CH<sub>4</sub>  
exchange in a temperate ombrotrophic bog. Atmos. Environ. 89, 249-259, 2014.
- Lai, D. Y. F., Roulet, D. N. T., Humphreys, E. R., Moore, T. R., Dalva, M.: The effect of atmospheric  
turbulence and chamber deployment period on autochamber CO<sub>2</sub> and CH<sub>4</sub> flux measurements  
in an ombrotrophic peatland. Biogeosciences 9, 3305-3322, 2012.



- 420 Limpens, J., Berendse, F., Blodau, C., Canadell, J. G., Freeman, C., Holden, J., Roulet, N., Rydin, H., Schaeppman-Strub, G.: Peatlands and the carbon cycle: from local processes to global implications—a synthesis. *Biogeosciences* 5, 1475-1491, 2008.
- Maeck, A., Hofmann, H., Lorke, A.: Pumping methane out of aquatic sediments – ebullition forcing mechanisms in an impounded river. *Biogeosciences* 11, 2925-2938, 2013.
- 425 Miller, L. G., Oremland, R. S.: Methane efflux from the pelagic regions of four lakes. *Glob. Biogeochem. Cycle* 2, 269-277, 1998.
- Ostrovsky, I., McGinnis, D. F., Lapidus, L., Eckert, W.: Quantifying gas ebullition with echo sounder: the role of methane transport by bubbles in a medium-sized lake. *Limnol. Oceanogr. Meth.* 6, 105-118, 2008.
- 430 Prairie, Y. T., del Giorgio, P. A.: A new pathway of freshwater methane emissions and the putative importance of microbubbles. *Inland Waters* 3, 311-320, 2013.
- Ramos, F. M., Lima, I. B. T., Rosa, R.R., Mazzi, E. A., Carvalho, J. C., Rasera, M. F. F. L., Ometto, J. P. H. B., Assireu, A. T., Stech, J. L.: Extreme event dynamics in methane ebullition fluxes from tropical reservoirs. *Geophys. Res. Lett.* 33, 1-4, 2006.
- 435 Repo, M. E., Huttunen, J. T., Naumov, A. V., Chichulin, A. V., Lapshina, E. D., Bleuten, W., Martikainen, P. J.: Release of CO<sub>2</sub> and CH<sub>4</sub> from small wetland lakes in western Siberia. *Tellus Ser. B-Chem. Phys. Meteorol.* 59, 788-796, 2007.
- Sahlée, E., Rutgersson, A., Podgrajsek, E., Bergström, H.: Influence from surrounding Land on the turbulence measurements above a lake. *Bound.-Layer Meteor.* 150, 235-258, 2014.
- 440 Savage, K., Phillips, R., Davidson, E.: High temporal frequency measurements of greenhouse gas emissions from soils. *Biogeosciences* 11, 2709-2720, 2014.
- Schrier-Uijl, A. P., Veraart, A. J., Leffelaar, P. A., Berendse, F., Veenendaal, E. M.: Release of CO<sub>2</sub> and CH<sub>4</sub> from lakes and drainage ditches in temperate wetlands. *Biogeochemistry* 102, 265-279, 2011.
- 445 Tokida, T., Miyazaki, T., Mizoguchi, M., Nagata, O., Takakai, F., Kagemoto, A., Hatano, R.: Falling atmospheric pressure as a trigger for methane ebullition from peatland. *Glob. Biogeochem. Cycle* 21, 1-8, 2007.
- Van der Nat, F. W., Middelburg, J.: Methane emission from tidal freshwater marshes. *Biogeochemistry* 49, 103-121, 2000.
- 450 Walter, K. M., Zimov, S. A., Chanton, J. P., Verbyla, D., Chapin III, F. S.: Methane bubbling from siberian thaw lakes as a positive feedback to climate warming. *Nature* 443, 71-75, 2006.



- Walter, K. M., Chanton, J. P., Chapin III, F. S., Schuur, E. A. G., Zimov, S. A.: Methane production and bubble emissions from arctic lakes: Isotopic implications for source pathways and ages. *J. Geophys. Res.* 113, 1-16, 2008.
- 455 Walter, K. M., Smith, L. C., Chapin III, F. S.: Methane bubbling from northern lakes: present and future contributions to the global methane budget. *Phil. Trans. R. Soc. A.* 365, 1657-1676, 2015.
- Whiting, G. J., Chanton, J. P.: Control of the diurnal pattern of methane emission from emergent aquatic macrophytes by gas transport mechanisms. *Aquat. Bot.* 54, 237-253, 1996.
- 460 Wik, M., Crill, P. M., Varner, R. K., Bastviken, D.: Multiyear measurements of ebullitive methane flux from three subarctic lakes. *J. Geophys. Res. Biogeosci.* 118, 1307-1321, 2013.
- Wik, M., Crill, P. M., Bastviken, D., Danielsson, A., Norbäck, E.: Bubbles trapped in arctic lake ice: Potential implications for methane emissions. *J. Geophys. Res.* 116, 1-10, 2011.
- Wille, C., Kutzbach, L., Sachs, T., Wagner, D., Pfeiffer, E.-M.: Methane emissions from Siberian arctic polygonal tundra: eddy covariance measurements and modeling. *Glob. Change Biol.* 14, 1395-1408, 2008.
- 465 Yu, Z., Slater, L. D., Schafer, K. V. R., Reeve, A. S., Varner, R. K.: Dynamics of methane ebullition from a peat monolith revealed from a dynamic flux chamber system. *J. Geophys. Res. Biogeosci.* 119, 1789-1806, 2014.
- 470



**Fig.1:** Transect of automatic chambers (AC) established at the measurement site. The arrow  
475 indicates the position of the climate station near chamber II.

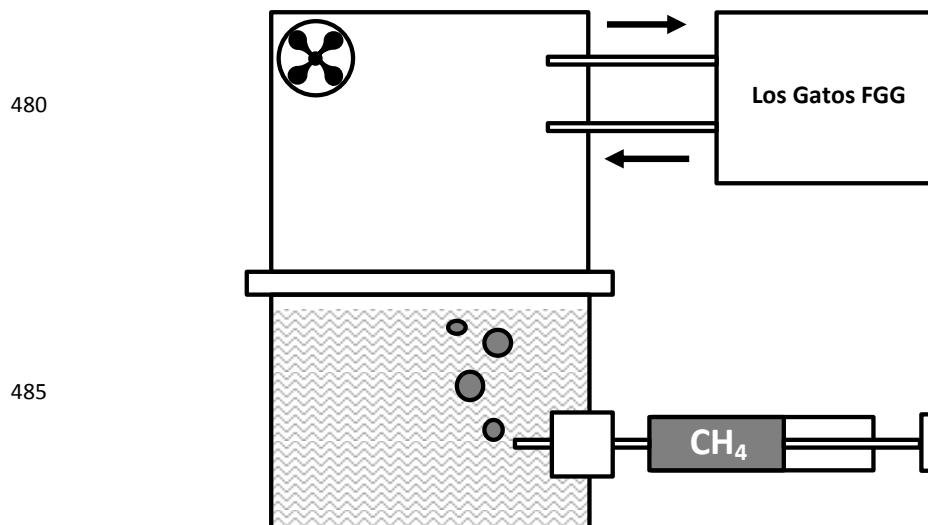


**Fig.2:** Scheme of experimental setup used for the simulation and determination of ebullition events with a Los Gatos Fast Greenhouse Gas (FGG) Analyser (911-0010, Los Gatos). The crimped area represents water filled tub. Injections of gaseous mixture (25000 ppm  $\text{CH}_4$  within artificial air; Linde, Germany) amounted to 5, 10, 20, 30 and 50 ml.

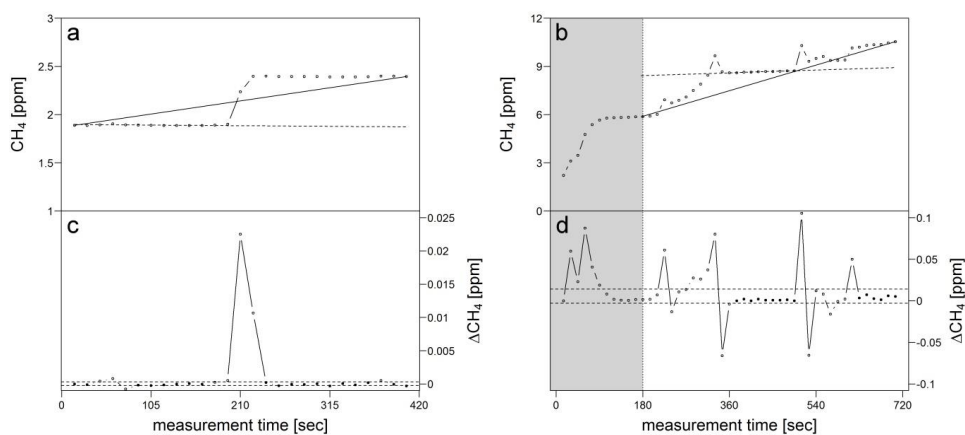


**Fig.3:** Scatterplots of recorded concentrations (ppm) within the chamber headspace for (a) a  
495 simulated ebullition event and (b) an exemplary  $\text{CH}_4$  measurement. The respective total  $\text{CH}_4$   
emission rate is represented by the black solid line, whereas  $\text{CH}_4$  released by diffusion is  
shown as a dashed line. The calculation of the corresponding diffusive flux is based on (c-d)  
concentration changes (ppm) between measurement points. Time spans dominated by  
diffusive  $\text{CH}_4$  release are marked by black dots, enclosed by the 25 % and 75 % quantiles  $\pm$   
500 0.25 IQR of obtained concentration changes, shown as black dashed lines. Unfilled dots  
outside the dashed lines display ebullition events (see also Goodrich et al. 2011; Miller and  
Oremland 1988). Gray shaded areas indicate the applied deathband (field study) at the  
beginning of each measurement (25%).

505

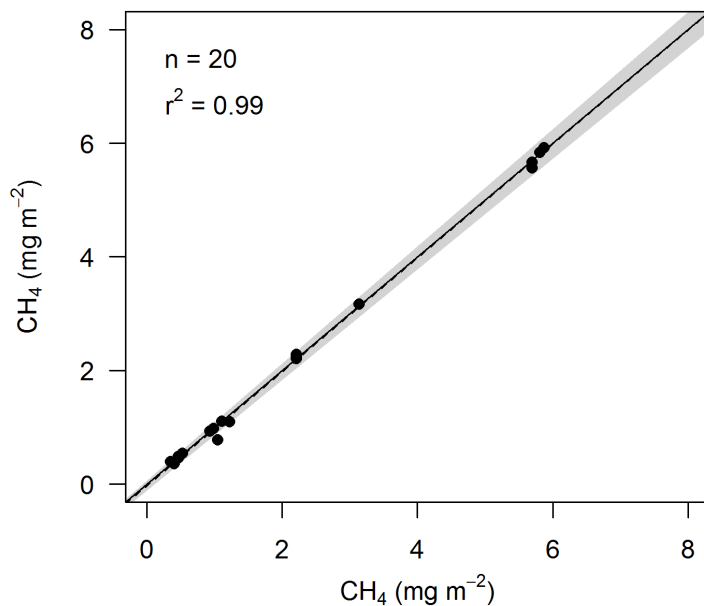
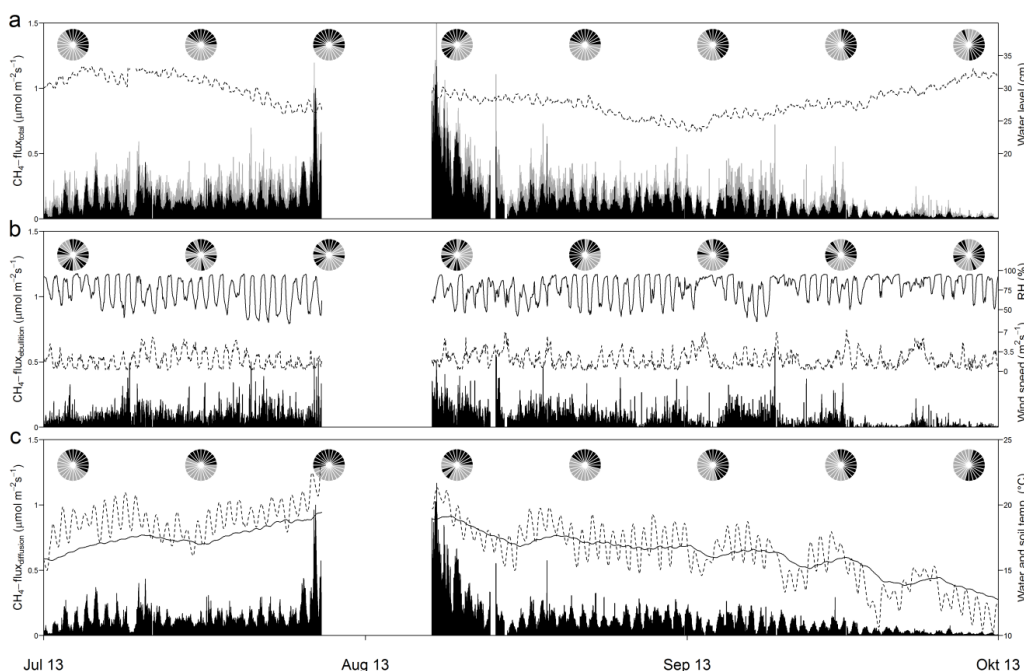


**Fig. 4:** Scatterplot of the amount of injected CH<sub>4</sub> and the corresponding calculated CH<sub>4</sub> ebullition event. The solid black line indicates the 1:1 agreement. The linear fit between the displayed values is represented by the black dashed line, surrounded by the 95% confidence interval (grey shaded area).

510



512

513 **Fig. 5:** Time series of (a) total CH<sub>4</sub> emissions and the corresponding amount of CH<sub>4</sub> released  
514 via (b) ebullition and (c) diffusion during the study period from July until September 2013.  
515 Development of important environmental parameters assumed to explain dynamics are also  
516 shown ((a) water level, (b) RH and wind speed and (c) sediment (solid line) and water  
517 temperature (dashed line)). Pie charts represent the biweekly pooled diurnal cycle of  
518 measured CH<sub>4</sub> fluxes. Slices are applied clockwise, creating a 24-hour clock, with black and  
519 light grey slices indicating hours with CH<sub>4</sub> flux above and below the daily mean, respectively.

520

521

522

523

524

525

526

527



528

529

530

531

532

533

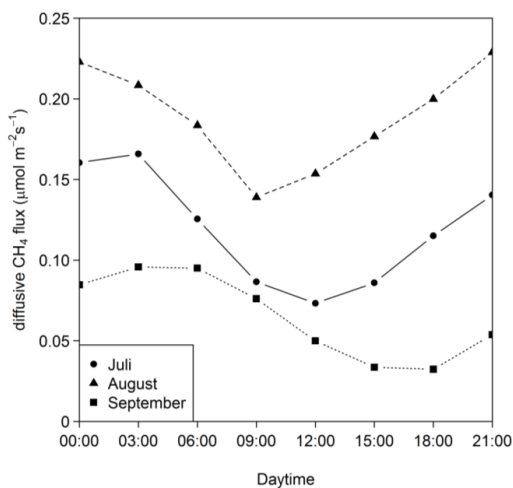
534

535

536

537

538



539 **Fig. 6:** Monthly averaged diurnal cycle of diffusive CH<sub>4</sub> fluxes indicating differences in  
540 magnitude and amplitude as well as a shift in minimum and maximum daily CH<sub>4</sub> fluxes over  
541 the turn of the study period.

542

543

544

545

546

547

548

549

550

551

552

553



554 **Tab. 1:** Monthly averages  $\pm$  1 standard deviation of hourly  $\text{CH}_4$  emissions ( $\text{mg m}^{-2} \text{h}^{-1}$ ) for the  
 555 chamber transect (from chamber I-IV, starting near the shoreline). Average standardized  
 556 (beta) coefficients and Nash-Sutcliffe's-Efficiency (NSE) based on linear regressions and  
 557 multiple linear regressions between different environmental drivers and daily subsets of  
 558 calculated  $\text{CH}_4$  emissions are shown below. Monthly averages as well as statistics are  
 559 separated according to diffusion, ebullition and total  $\text{CH}_4$  flux. Superscript numbers indicate  
 560 significant differences between chambers. p-values of applied linear and multiple linear  
 561 regressions are indicated via asterisks.

Month	Chamber	$\text{CH}_4_{\text{diffusion}}$	$\text{CH}_4_{\text{ebullition}}$	$\text{CH}_4_{\text{total}}$
		$\text{mg m}^{-2} \text{h}^{-1}$		
July	I	$4.6^{24} \pm 3.1$	$5.5 \pm 7.0$	$10.1^{24} \pm 7.8$
	II	$1.8^{134} \pm 1.5$	$3.7 \pm 6.9$	$5.5^{134} \pm 7.1$
	III	$6.1^{24} \pm 4.0$	$4.7 \pm 6.9$	$10.7^{24} \pm 8.2$
	IV	$8.7^{123} \pm 5.9$	$4.7 \pm 5.3$	$13.3^{123} \pm 7.6$
August	I	$5.1 \pm 5.9$	$5.0^{24} \pm 6.8$	$10.1 \pm 10.0$
	II	$3.7 \pm 5.0$	$2.9^{14} \pm 6.0$	$6.5 \pm 8.6$
	III	$5.7 \pm 4.9$	$5.8^{24} \pm 7.4$	$11.5 \pm 9.5$
	IV	$6.1 \pm 6.8$	$3.0^{13} \pm 5.0$	$9.1 \pm 9.4$
September	I	$2.3^{24} \pm 2.0$	$1.8^{24} \pm 3.9$	$4.1^{24} \pm 4.8$
	II	$2.6^1 \pm 2.7$	$1.1^{13} \pm 3.0$	$3.7^{13} \pm 4.4$
	III	$3.9^4 \pm 3.9$	$5.4^{24} \pm 6.9$	$9.3^{24} \pm 8.8$
	IV	$1.3^{13} \pm 1.6$	$0.7^{13} \pm 3.4$	$2.1^{13} \pm 4.0$
Mean	$5.1 \pm 5.7$	$4.2 \pm 6.5$	$9.2 \pm 9.6$	
Driver	$\text{CH}_4_{\text{diffusion}}$	$\text{CH}_4_{\text{ebullition}}$	$\text{CH}_4_{\text{total}}$	
	average standardized (beta) coefficient of daily data subsets			
wind velocity	-0.4 <sup>ˆ</sup>	-0.1	-0.3 <sup>ˆ</sup>	
relative humidity (RH)	0.5*	0.1	0.4 <sup>ˆ</sup>	
Air pressure	0.0	-0.1	0.0	
water level	-0.5*	-0.1	-0.4 <sup>ˆ</sup>	
air temp. (2 m)	-0.6*	-0.1	-0.4 <sup>ˆ</sup>	
water temp. (5 cm)	0.1 <sup>ˆ</sup>	0.1	0.1 <sup>ˆ</sup>	
sediment temp. (2 cm)	0.3 <sup>ˆ</sup>	0.0	0.2 <sup>ˆ</sup>	
$\Delta$ water-air temp.	0.6*	0.1	0.4 <sup>ˆ</sup>	
average NSE of MLR	0.72	0.30	0.51	

<sup>1234</sup> significant difference ( $\alpha=0.1$ ) between chamber I (1), II (2), III (3) and IV(4)

<sup>ˆ</sup>\* significant dependency with average p-value < 0.2 and p-value < 0.1